Phosphorylation of the RGS Protein Sst2 by the MAP Kinase Fus3 and Use of Sst2 as a Model To Analyze Determinants of Substrate Sequence Specificity†

Stephen C. Parnell,¥ Louis A. Marotti, Jr.,‡,¥ Lee Kiang,§ Matthew P. Torres, Christoph H. Borchers, and Henrik G. Dohlman*

Department of Biochemistry and Biophysics, University of North Carolina, Chapel Hill, North Carolina

Received February 19, 2005; Revised Manuscript Received April 4, 2005

ABSTRACT: Previously, we used mass spectrometry to demonstrate pheromone-stimulated phosphorylation of Ser-539 in Sst2, a regulator of G protein signaling in yeast *Saccharomyces cerevisiae* [Garrison, T. R., et al. (1999) *J. Biol. Chem*. *274*, 36387−36391]. Here, we show that Sst2 phosphorylation is mediated by the mitogen-activated protein (MAP) kinase Fus3. Phosphorylation occurs within a canonical MAP kinase phosphorylation site (Pro-X-Ser/Thr-Pro, where "X" at the −1 position can be any amino acid), a consensus sequence deduced earlier from analysis of synthetic peptide substrates. In a direct test of the model, we compared Sst2 phosphorylation following systematic substitution of the −1 residue His-538. Each of the substitution mutants was suitable as a MAP kinase substrate, as shown by phosphorylation-dependent mobility shifts in vivo and/or by direct phosphorylation in vitro followed by peptide mapping and mass spectrometry sequencing. This analysis documents phosphorylation of Sst2 by Fus3 and demonstrates that the prevailing model for MAP kinase recognition is valid for a native substrate protein in vivo as well as for small synthetic peptides tested in vitro.

Many external signals exert their effects by binding to cell surface receptors linked to G proteins. In humans, G protein-coupled receptors mediate the effects of hormones and neurotransmitters, as well as sensory stimuli such as odors, taste, and light. In yeast *Saccharomyces cerevisiae*, G proteins transmit a signal leading to mating. In this example, pheromones bind to a cell surface receptor (Ste2), which promotes GTP binding to the G protein α subunit (Gpa1). Gpa1 then dissociates from the G$\beta\gamma$ subunit dimer (Ste4/Ste18), and the dissociated components propagate the signal through a variety of effector proteins (*1*). Upon GTP hydrolysis, the G protein subunits reassociate and signaling stops. This inactivation step is mediated in part by Sst2, a regulator of G protein signaling (RGS[1] protein) that accelerates GTPase activity and thereby promotes subunit reassembly (*2*, *3*).

Of the known effectors in the pheromone pathway, the best-characterized is a multiprotein complex comprised of Ste5, Ste11, Ste7, and Fus3. Fus3 is a MAP kinase, which is phosphorylated and activated by Ste7. Ste7 is itself phosphorylated and activated by Ste11. Ste5 serves as a scaffold to assemble all three kinases and is recruited to the plasma membrane by the activated G protein. A second MAP kinase called Kss1 does not normally bind to Ste5 but appears able to transmit the mating signal in the absence of Fus3 (*4*).

In yeast, Fus3 is known to phosphorylate a transcription activator (Ste12) (*5*−*8*), transcription repressors (Dig1/Rst1, Dig2/Rst2) (*8*, *9*), the upstream kinase (Ste7) (*10*, *11*), a MAP kinase phosphatase (Msg5) (*12*, *13*), an inhibitor of the G1 cyclin-Cdc28 kinase (Far1) (*5*, *6*, *8*, *14*, *15*), and a Ras guanine nucleotide exchange factor (Cdc25) (*16*). There is also indirect evidence that Fus3 can phosphorylate receptors (Ste3) (*17*), the G protein β subunit (Ste4) (*18*), Ste5 (*5*, *12*, *19*), and Sst2 (*20*). Previously, we observed that Sst2 from pheromone-treated cells undergoes an electrophoretic mobility shift that can be readily detected by immunoblotting. We purified the modified form of Sst2 and used electrospray ionization mass spectrometry to detect phosphorylation at Ser-539. This residue lies within an ideal consensus MAP kinase phosphorylation site: Pro-X-Ser/Thr-Pro, where "X" can be any amino acid, and either Ser or Thr can be modified by phosphorylation (*21*, *22*). Phosphorylation was blocked by deletion of the genes that encode the MAP kinases (*FUS3* and *KSS1*) or other components needed for MAP kinase activation (*STE11*, *STE7*, *STE4*, and *STE18*). Phosphorylation was likewise blocked by replacing Ser-539 with Ala, Asp, or Glu (but not Thr) (*20*).

Although a slower rate of degradation was noted for the phosphorylated versus nonphosphorylated species, point mutations at Ser-539 did not alter pheromone sensitivity (*20*).

† This work was supported by National Institutes of Health Grants ES011997 (to C.H.B.), GM055316, and GM059167 (to H.G.D.).

* Address correspondence to Henrik G. Dohlman, Ph.D., Department of Biochemistry and Biophysics, University of North Carolina at Chapel Hill, 405 Mary Ellen Jones Building, Campus Box 7260, Chapel Hill, NC 27599-7260. Phone: (919) 843-6894. Fax: (919) 966-2852. E-mail: hdohlman@med.unc.edu.

¥ These authors contributed equally.

‡ Present address: Department of Neurosurgery, Yale University School of Medicine, New Haven, CT 06536.

§ Present address: Cornell/Rockefeller/Sloan-Kettering Tri-Institutional MD-PhD Program, Weill Medical College of Cornell University, New York, NY 10021.

[1] Abbreviations: RGS, regulator of G protein signaling; SDS−PAGE, sodium dodecyl sulfate−polyacrylamide gel electrophoresis; MAP, mitogen-activated protein; HPLC, high-performance liquid chromatography; MALDI, matrix-assisted laser desorption ionization; TOF, time-of-flight.

10.1021/bi0503091 CCC: $30.25
Published on Web 05/10/2005

The absence of any functional effect of phosphorylation is consistent with the crystal structure of rat $G_{i1}\alpha$ complexed with RGS4 (*23*), which reveals that Ser-539 in Sst2 would be located on the side of the RGS domain opposite that which interacts with the G protein, and should not therefore directly affect the Sst2−Gpa1 interaction. Correspondingly, Sst2 could undergo phosphorylation even in the Gpa1-bound state (*20*).

These earlier findings suggested that the G protein-regulated MAP kinase promotes feedback phosphorylation of Sst2 after pheromone treatment. Here, we demonstrate that Fus3 phosphorylates Sst2 directly. Further examination of the substrate sequence specificity for Fus3 phosphorylation of Sst2 reveals no preferred amino acid at the −1 position. This result demonstrates that the consensus sequence deduced from analysis of short synthetic peptides is valid as well for a native, full-length protein substrate.

EXPERIMENTAL PROCEDURES

Strains and Plasmids. The *S. cerevisiae* strain used in this study was YDM400 (*MAT**a** ura3-52 lys2-801*^{am} *ade2-101*^{oc} *trp1-*Δ*63 his3-*Δ*200 leu2-*Δ*1 sst2-*Δ*2*) (*24*).

Yeast cells were transformed using the Quick and Easy TRAFO protocol (*25*). Plasmid pAD4M-SST2-his was constructed by replacing the BssHII−HindIII fragment of *SST2* in pAD4M (*26*) with the corresponding sequence from pQE60-SST2-his (*2*). Plasmid pET11d-his-SST2 was kindly provided by Lorena Kallal and Rick Fishel (*27*). Plasmid pGEX-2T6-FUS3 was generously provided by Beverly Errede (*28*). *SST2* and *FUS3* mutants were obtained using the Stratagene QuikChange Site-Directed Mutagenesis Kit according to the manufacturer's directions.

Mutagenic primers used to construct *FUS3*^{K42R} were (5′ CCACG GGAGA AATCG TGGCA ATCCG GAAGA TCGAA CCATT CGATA AGCCT TTG 3′), *SST2*^{S539A} (5′ CTGAC ATCAT GTTGC ACCCT CATAC GCCCT TATCG GAACA CTTTC C 3′), *SST2*^{H538D} (5′ CATGT TGCAC CCTGA TTCTC CATTA TCG 3′), *SST2*$^{H538\Delta}$ (5′ CTGAC ATCAT GTTGC ACCCT ___TC TCCAT TATCG GAACA C 3′), and *SST2*^{H538A} (5′ CTGAC ATCAT GTTGC ACCCT GCTTC TCCAT TATCG GAACA C 3′). Complementary primers are not shown. The remaining mutagenic primers were generated using the H538A mutant as the template, with the underlined bases replaced as follows: TGT (C), GAA (E), TTT (F), GGT (G), ATT (I), AAA (K), TTG (L), ATG (M), AAT (N), CCA (P), CAA (Q), AGA (R), TCT (S), ACT (T), GTT (V), TGG (W), and TAT (Y). Mutations were verified by DNA sequencing and also confirmed by restriction digestion analysis whenever possible (*FUS3*^{K42R} mutagenic primers introduce a BspEI site, and *SST2*^{H538R} introduces a BglII site).

Preparation of Whole Cell Lysates and Immunoblotting. Cells were grown at 30 °C in selective media to mid-log phase and treated with 2.5 μM α-factor pheromone for 1 h, unless otherwise indicated. Cells were harvested by centrifugation at 2000*g* for 10 min at 4 °C, washed in cold 10 mM NaN_3, recentrifuged, then resuspended (1.5×10^6 cells/μL) in SDS−polyacrylamide gel electrophoresis (SDS−PAGE) sample buffer (62.5 mM Tris-HCl, pH 6.8, 10% glycerol, 2% SDS, 1% 2-mercaptoethanol, and 0.0005% bromophenol blue), and boiled for 10 min. The cells were disrupted by glass bead vortex homogenization (Sigma, G-8772) for 4 min and centrifuged at 16 000*g* for 2 min. The supernatant was collected and stored at −20 °C. Lysates were reheated at 37 °C for 10 min then resolved by 6.5 or 8% SDS−PAGE. Proteins were transferred to nitrocellulose by electrophoresis, probed with anti-Sst2 (*24*) or Tetra-His (Qiagen) antibodies, and tracked by enhanced chemiluminescence detection (Perkin-Elmer) according to manufacturer's specifications.

Purification of His-Sst2. Plasmid pET11d containing *SST2* variants (WT, S539A, H538A, H538F, H538P, H538Q, or H538W) were transformed into *Escherichia coli* BL21(DE3) pLysS cells (Novagen). Single colonies were grown overnight with shaking at 37 °C in Luria−Broth supplemented with 50 μg/mL carbenicillin. The overnight culture was diluted 1:33 into fresh media and grown at 37 °C with shaking to a $A_{600\ nm} \sim 0.5-0.6$ (∼1.5 h), followed by an additional 0.5 h at 30 °C with shaking. Fusion protein expression was induced by the addition of isopropyl β D-thiogalactopyranoside to a final concentration of 1 mM followed by 2.5 h at 30 °C with shaking. Following induction, cells were chilled, harvested by centrifugation (5 min, 4500*g* at 4 °C in a Sorvall GS-3 rotor), and resuspended in ice-cold buffer A (50 mM Hepes, 300 mM NaCl, and 10% glycerol, pH 8.0). Cells were homogenized using an Emulsiflex-C5 Homogenizer (AVESTIN). The resulting lysate was clarified twice by centrifugation (15 min, 12 000*g* at 4 °C in a Sorvall SS-34 rotor). TALON Superflow Metal Affinity Resin (BD Biosciences) was washed three times with buffer A and added to the clarified lysate. Fusion proteins were bound at room temperature for 45 min with gentle agitation, followed by 5 min, 500*g*, 4 °C centrifugation in a Sorvall Legend RT Tabletop centrifuge. The supernatant was discarded, and fusion proteins were washed three times with 50 bead volumes of cold buffer A by gentle agitation for 15 min at room temperature, followed by centrifugation. Fusion proteins were eluted with three stepwise gradients of imidazole (83.3, 166.7, and 250 mM) in 2 bead volumes of buffer A, followed by a final elution in 1 bead volume of 250 mM imidazole in buffer A. The eluate was pooled and dialyzed into buffer B (50 mM Hepes, 0.1 mM EDTA, 1 mM DTT, 150 mM NaCl, and 10% glycerol, pH 8.0). Fusion protein was stored at 4 °C.

Purification of GST-MAP Kinases. Plasmid pGEX-2T6 containing MAP kinase variants (*FUS3* and *FUS3*^{K42R}) were transformed into *E. coli* BL21(DE3) cells. Single colonies were grown overnight with shaking at 37 °C in Luria−Broth supplemented with 50 μg/mL carbenicillin. The overnight culture was diluted 1:11 into fresh media and grown at 37 °C for 0.5 h with shaking, followed by an additional 0.75 h at room temperature with shaking. Fusion protein expression was induced by the addition of isopropyl β D-thiogalactopyranoside to a final concentration of 0.1 mM followed by 5 h at room temperature with shaking. Following induction, cells were chilled, harvested by centrifugation (10 min, 4500*g*, 4 °C in a Sorvall GS-3 rotor), and resuspended in ice-cold buffer C (150 mM NaCl, 16 mM Na_2HPO_4, and 4 mM NaH_2PO_4, pH 7.3). Cells were homogenized using an Emulsiflex-C5 Homogenizer (AVESTIN). Triton X-100 was added to a final concentration of 1%, and the lysate was clarified twice by centrifugation (15 min, 12 000*g* at 4 °C in a Sorvall SS-34 rotor). Glutathione Sepharose 4B (Am-

ersham Pharmacia Biotech AB) was washed three times with buffer C and added to the clarified lysate. Fusion proteins were bound at room temperature for 45 min with gentle agitation, followed by 5 min, 500*g* at 4 °C in a Sorvall Legend RT Tabletop centrifuge. The supernatant was discarded, and fusion proteins were washed three times with 50 bead volumes of cold buffer C by gentle agitation for 5 min at room temperature, followed by centrifugation. Fusion proteins were eluted three times with 1 bead volume of 5 mM reduced glutathione in 50 mM Tris-HCl, pH 7.5. The eluate was pooled and dialyzed into buffer D (25 mM Hepes, 15 mM $MgCl_2$, 5 mM EGTA, and 1 mM $MnCl_2$, pH 7.2). Following dialysis, glycerol was added to a final concentration of 15%, and the fusion protein was stored at −20 °C.

In Vitro Kinase Assay. GST-MAP kinase fusion protein was incubated in kinase buffer (25 mM Hepes, 15 mM $MgCl_2$, 5 mM EGTA, 1 mM $MnCl_2$, 3.5 mM DTT, and 210 μM ATP, pH 7.2) with Protease Inhibitor Cocktail (Sigma P8215) at 0.3% (v/v) at 30 °C for 0.75 h. Sst2 substrate was added, and ATP was increased to a final concentration of 300 μM. Following incubation (3 h, unless indicated), the reaction was terminated by the addition of 6× SDS−PAGE sample buffer. Samples were boiled 4 min and then resolved by SDS−PAGE and detected by immunoblotting as described above. For samples to be detected by autoradiography, Sst2 substrate was incubated with 6 μCi [γ-^{32}P]-ATP, 3000 Ci/mmol (Perkin-Elmer). Following electrophoretic transfer, ^{32}P-incorporation was detected using a PhosphorImager SI (Molecular Dynamics). For samples to be analyzed by peptide mapping and mass spectrometry, Sst2 substrate was incubated with 17 μCi [γ-^{32}P]-ATP and prepared as described below.

Peptide Mapping and Mass Spectrometry. Preparation of Sst2 for mass spectrometric analysis was accomplished by separation on a 4−12% Bis-Tris NuPAGE precast gel (Invitrogen) in 1× MOPS running buffer followed by in-gel digestion with porcine trypsin (Promega) as described previously (*29*). The extracted peptides were diluted to 5% acetonitrile with high-performance liquid chromatography (HPLC)-grade water and fractionated by reverse-phase HPLC (HP1100, Agilent Technologies) using a Vydac C_{18}-MS column (250 mm × 4.6 mm). Peptides were eluted from the column using a 60 min linear gradient of 5−65% acetonitrile in 0.1% trifluoroacetic acid at 1 mL/min). Fractions were collected in 1 mL volumes for 50 min, frozen, and lyophilized. Lyophilized fractions were reconstituted in 5 μL of 80% acetonitrile/0.1% trifluoroacetic acid and analyzed by matrix-assisted laser desorption ionization time-of-flight mass spectrometry (MALDI-TOF MS). Briefly, 0.3 μL of the reconstituted fraction was applied to a MALDI target plate with an equivalent volume of saturated α-cyano-4-hydroxycinnamic acid in 50% acetonitrile/0.1% trifluoroacetic acid. Spots were dried at room temperature and then analyzed using a Bruker Daltonics Reflex III MALDI-TOF instrument operating in linear mode. Alternatively, $^1/_{10}$ of the fractions were used for scintillation counting of ^{32}P-labeled peptides using an LS 6500 Multi-Purpose Scintillation Counter (Beckman Coulter).

Pheromone Response Assays. Growth arrest halo assays and reporter-transcription assays were performed as described previously (*30*).

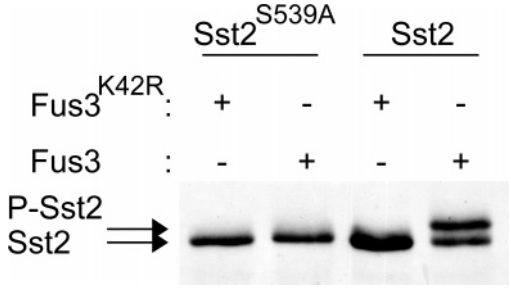

FIGURE 1: Sst2 is phosphorylated directly by Fus3. To determine whether Fus3 phosphorylates Sst2, wild-type or phosphorylation-site mutant Sst2^{S539A} were purified from *E. coli* and used as substrates for recombinant Fus3 in an in vitro kinase reaction. To verify that phosphorylation is mediated by Fus3 and not a contaminating kinase, the same experiment was performed using a catalytically inactive mutant, Fus3^{K42R}. Fus3 fusion proteins were activated by a 45 min preincubation with ATP. The conversion of Sst2 to the phosphorylated species ("P-Sst2") was monitored by 6.5% SDS−PAGE and immunoblotting, using anti-Tetra-His antibodies.

RESULTS

We demonstrated previously that Sst2 is phosphorylated in response to pheromone stimulation and that this phosphorylation occurs at Ser-539. On the basis of the location of this Ser within an ideal MAP kinase consensus sequence and the loss of phosphorylation in MAP kinase mutants (gene deletion and kinase-inactivating mutations), we concluded that Fus3 most likely mediates the phosphorylation of Sst2 (*20*). To test this directly, we sought to measure phosphorylation of Sst2 using purified recombinant proteins in an in vitro kinase reaction. By purifying Fus3 and Sst2 from bacteria, we could exclude the possibility that Sst2 is phosphorylated by an unknown yeast kinase that is itself activated by a MAP kinase. We could also rule out the possibility that kinase activity requires additional cofactors or post-translational modifications, since they would be absent in *E. coli*. As shown in Figure 1, purified Sst2 underwent a ∼2 kDa mobility shift upon incubation with purified and activated Fus3. The shift required Fus3 kinase activity, since Sst2 mobility was unaffected by incubation with the catalytically inactive mutant Fus3^{K42R}. Consistent with our previous observations (*20*), the mobility of Sst2 remained unaltered when Ser-539 was replaced with Ala (Sst2^{S539A}).

We then investigated the substrate sequence specificity for Fus3 phosphorylation; in particular, we focused on the residue at the −1 position, the amino acid that immediately precedes the phosphorylated Ser. The prevailing model states that MAP kinases do not distinguish between substrates that differ at the −1 position. While this model is consistent with the available data, it has never been explicitly tested in vivo and has never been tested in a comprehensive manner using a full-length native protein substrate. One reason is the lack of appropriate substrates. A rigorous test of the model would require identification of a protein for which (*a*) the phosphorylation site is clearly established in vivo, (*b*) the phosphorylation site adheres to the established consensus sequence, and (*c*) where phosphorylation of that site can be readily assayed both in vitro and in vivo. Sst2 may be the only protein that meets all of these requirements. Sst2 is a rare example of a MAP kinase substrate for which the in vivo phosphorylation site (Ser-539) has been mapped directly

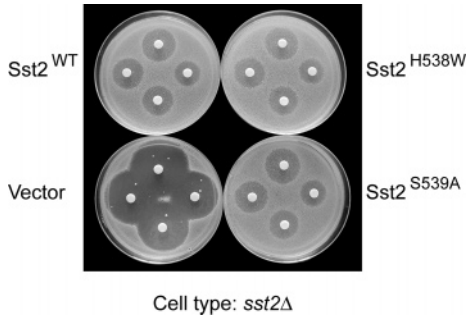

FIGURE 2: His-538 substitutions do not alter Sst2 activity. To demonstrate that $Sst2^{H538X}$ mutants were expressed, folded, and localized correctly, their ability to function in place of the wild-type Sst2 was determined using a growth arrest plate assay. YDM400 ("*sst2*Δ") cells transformed with plasmid pAD4M containing no insert ("vector"), wild-type *SST2* ("$Sst2^{WT}$"), the phosphorylation-site mutant ("$Sst2^{S539A}$"), or each of the His-538 mutants ($Sst2^{H538W}$ is shown, others were identical) were plated onto solid medium and exposed to 12.5, 25, 50, and 100 μg of α-factor spotted onto filter disks. The resulting zone of growth inhibition was documented after 2 days. Halo turbidity is due to constitutive expression of Sst2.

in yeast. Phosphorylation occurs within a perfect MAP kinase consensus sequence (Pro-His-Ser-Pro). Moreover, the phosphorylation of Ser-539 leads to an electrophoretic mobility shift of the protein, so the modification can be easily monitored by SDS−PAGE and immunoblotting. Finally, phosphorylation has no measurable effect on Sst2 function; therefore, mutations that alter Sst2 phosphorylation can be easily tested for proper folding and activity, through complementation of an *sst2*Δ gene deletion.

Having established that Sst2 is phosphorylated by Fus3, we investigated the substrate sequence specificity using $Sst2^{H538X}$ mutants as test substrates. Our experimental strategy was to test a panel of Sst2 mutants in which His-538 was replaced with 19 other amino acids or was deleted. To establish the functionality of the His-538 mutants, we expressed each in an *sst2*Δ mutant strain and tested their ability to restore normal pheromone responses. This was first done using the growth arrest plate assay. Cells expressing wild-type Sst2, $Sst2^{S539A}$, or each of the His-538 mutants were plated onto solid medium and exposed to 12.5, 25, 50, and 100 μg of α-factor spotted onto filter disks. The resulting zone of growth inhibition was documented after 2 days. Whereas cells lacking *SST2* (i.e., transformed with the empty vector) were considerably more responsive than the $SST2^{+}$ cells, all of the mutants responded precisely like the wild-type (Figure 2, and data not shown). We then evaluated each mutant using a reporter-transcription assay. We have shown previously that the absence of *SST2* does not appreciably alter the maximum response but rather results in a ~100-fold decrease in the concentration of α-factor necessary to achieve 50% of the maximum agonist response (EC_{50}) (*30*, *31*). Again, and in agreement with the results of the growth arrest assay, all of the His-538 mutations functioned precisely like wild-type Sst2 (Table 1).

The ability of each mutant to be phosphorylated in vivo was then monitored by immunoblotting. Wild-type Sst2 served as a positive control, and the phosphorylation-site mutant $Sst2^{S539A}$ served as a negative control. As shown in Figure 3, nearly all wild-type Sst2 was phosphorylated 1 h after kinase activation (pheromone treatment). Pheromone

Table 1: Reporter Transcription Activity in Cells that Express $Sst2^{H538X}$ Mutants

Sst2	Log EC_{50} (M)	Sst2	Log EC_{50} (M)
H538**A**	−4.98 ± 0.46	H538**N**	−5.11 ± 0.59
H538**C**	−5.02 ± 0.47	H538**P**	−5.23 ± 0.60
H538**D**	−5.11 ± 0.47	H538**Q**	−5.13 ± 0.60
H538**Δ**	−5.14 ± 0.47	H538**R**	−5.01 ± 0.46
H538**E**	−5.66 ± 0.61	H538**S**	−5.07 ± 0.58
H538**F**	−5.02 ± 0.49	H538**T**	−5.13 ± 0.47
H538**G**	−5.11 ± 0.47	H538**V**	−5.01 ± 0.59
H538**I**	−5.06 ± 0.58	H538**W**	−5.04 ± 0.60
H538**K**	−5.13 ± 0.47	H538**Y**	−5.09 ± 0.49
H538**L**	−5.14 ± 0.47	S539**A**	−4.98 ± 0.46
H538**M**	−5.16 ± 0.47	WT	−5.06 ± 0.47

treatment also led to increased phosphorylation of Sst2 when the His at the −1 position was substituted with another amino acid or was deleted. In some cases, the starting (basal) level of phosphorylation was reduced, but there was nevertheless a *pheromone-dependent* increase in phosphorylation. In addition and in contrast to wild-type Sst2, for many of the mutants, a significant portion of Sst2 remained unphosphorylated even following pheromone stimulation. Moreover, in some mutants, the difference in mobility of the two forms of the protein was barely discernible ($Sst2^{H538F}$ and $Sst2^{H538P}$) or was abolished altogether ($Sst2^{H538W}$). The negative control mutant $Sst2^{S539A}$ also failed to undergo a mobility shift, as expected.

We then sought to determine whether any changes in the phosphorylation state of $Sst2^{H538X}$ mutants were due to intrinsic differences in their ability to serve as Fus3 substrates. Alternatively, such differences could be due to external factors (for example, differences in phosphatase sensitivity). This distinction is important, since changes in the intrinsic ability of Sst2 to serve as a Fus3 substrate would contradict the prevailing model that the residue at −1 is interchangeable. Thus, we compared the ability of purified Fus3 to phosphorylate purified wild-type or representative mutants $Sst2^{H538A}$ (exhibits reduced basal phosphorylation) and $Sst2^{H538F}$ (exhibits a reduced mobility shift) over time. As shown in Figure 4, Fus3-mediated phosphorylation of Sst2 was unaltered by either substitution. While a significantly greater portion of $Sst2^{H538A}$ than wild-type remains unphosphorylated following pheromone treatment in vivo (see Figure 3), both forms of the protein were phosphorylated with similar kinetics in vitro. Thus, Fus3-dependent phosphorylation of $Sst2^{H538A}$ and $Sst2^{H538F}$ appears identical to that of wild-type Sst2 in vitro.

We then sought to determine whether the reduction or absence of a mobility shift by a subset of mutants was due to intrinsic differences in their ability to serve as Fus3 substrates or due simply to altered electrophoretic mobility. To this end, we compared the ability of the subset of mutants to incorporate ^{32}P in the presence of Fus3. Recombinant $Sst2^{H538F}$ (representative mutant used in Figure 4), $Sst2^{H538P}$, $Sst2^{H538W}$, $Sst2^{S539A}$ (negative control), and wild-type Sst2 (positive control), as well as $Sst2^{H538A}$ and $Sst2^{H538Q}$, were affinity-tagged, expressed in *E. coli*, and purified. As shown in Figure 5A, all $Sst2^{H538X}$ mutants tested were phosphorylated to the same extent as wild-type Sst2, which was phosphorylated ~4-fold more efficiently than $Sst2^{S539A}$. As expected, no ^{32}P was incorporated into wild-type Sst2 upon incubation with the catalytically inactive $Fus3^{K42R}$. Finally,

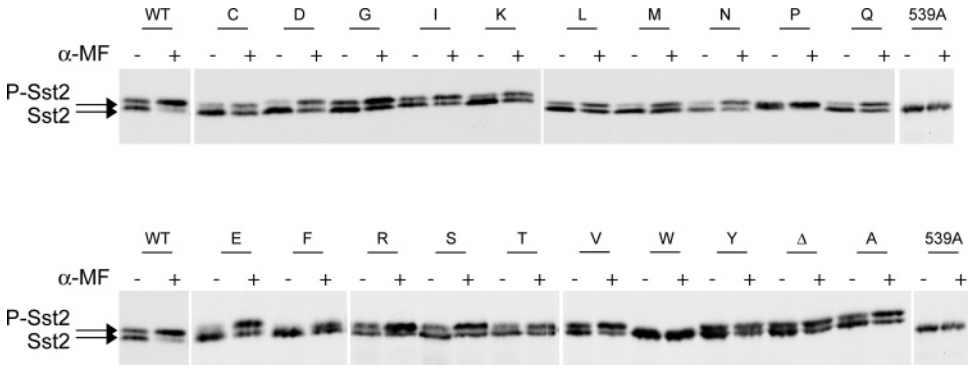

FIGURE 3: Effects of His-538 substitutions on the phosphorylation of Sst2 in vivo. To determine whether the residue at the −1 position (His-538) affects the ability of Sst2 to be phosphorylated by Fus3 in vivo, the electrophoretic mobility of each $Sst2^{H538X}$ mutant was determined with and without pheromone treatment. His-538 was deleted (Δ) or mutated to each of the 19 other amino acid residues (as indicated by single letter code). Wild-type ("WT") and Ser-539-Ala mutant ("539A") Sst2 were used as a positive and negative control, respectively. Sst2 mutants were expressed using plasmid pAD4M in an *sst2*Δ mutant strain, YDM400. Plasmid pAD4M contains a constitutive promoter from *ADH1*, used to produce equal Sst2 expression under pheromone-induced and -uninduced conditions. Cells were grown to mid-log phase and then treated with ("+") or without ("−") 2.5 μM α-mating factor ("α-MF") for 1 h to promote Sst2 phosphorylation. Cells were subsequently lysed in SDS−PAGE sample buffer, and the conversion of Sst2 to the slower-migrating phosphorylated species ("P-Sst2") was monitored by 8% SDS−PAGE and immunoblotting, using anti-Sst2 antibodies.

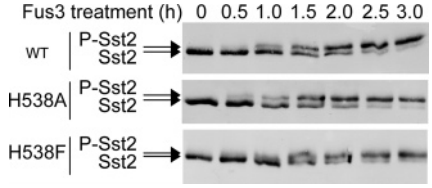

FIGURE 4: His-538 substitutions do not alter the kinetics of Sst2 phosphorylation in vitro. To determine whether substitution at His-538 affects Sst2 phosphorylation kinetics, bacterially expressed and purified Fus3 was mixed with bacterially expressed and purified wild-type Sst2 or representative mutants $Sst2^{H538A}$ (exhibits reduced basal phosphorylation) and $Sst2^{H538F}$ (exhibits a reduced mobility shift). Sst2 proteins were incubated for the times indicated with preactivated Fus3, and the reactions were terminated by the addition of 6× SDS−PAGE sample buffer and boiling. The conversion of Sst2 to the slower migrating phosphorylated species ("P-Sst2") was monitored by 6.5% SDS−PAGE and immunoblotting, using anti-Tetra-His antibodies.

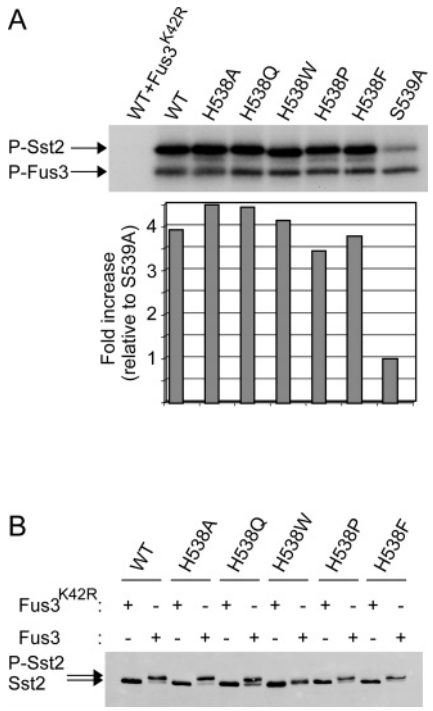

FIGURE 5: His-538-Trp substitution blocks the phosphorylation-dependent mobility shift but preserves phosphorylation of Sst2. (A) To determine whether substitutions at His-538 affect Sst2 phosphorylation in vitro, bacterially expressed and purified wild-type or representative Sst2 mutants (H538A, H538Q, H538W, H538P, H538F, and S539A) were mixed with bacterially expressed and purified Fus3 and [^{32}P-γ]-ATP in an in vitro kinase reaction. Conversion of Sst2 to the phosphorylated species ("P-Sst2") was monitored by 6.5% SDS−PAGE and phosphorimaging. The level of $Sst2^{H538X}$ phosphorylation is expressed as a fold-increase in the amount of ^{32}P incorporation relative to the $Sst2^{S539A}$ mutant. (B) To confirm that each mutant exhibits the same differences in mobility when phosphorylated in vitro as in vivo, the purified proteins were phosphorylated using nonradioactive phosphate. The conversion of Sst2 to the phosphorylated species ("P-Sst2") was monitored by 6.5% SDS−PAGE and immunoblotting, using anti-Tetra-His antibodies.

we wished to confirm that each of these mutants exhibits the same differences in mobility when phosphorylated in vitro as they do in vivo. In this case, each purified protein was phosphorylated using nonradioactive phosphate. When examined by the electrophoretic mobility shift assay (Figure 5B), all of the $Sst2^{H538X}$ mutants tested underwent a mobility shift very similar to that observed in vivo (Figure 3).

Having demonstrated that $Sst2^{H538W}$ is indeed phosphorylated by Fus3, we sought to confirm that this and other mutants are still phosphorylated at Ser-539. ^{32}P-Labeled Sst2 fusion proteins were trypsinized, and the resulting peptides were separated by C18 reverse-phase HPLC. Fractions were collected and analyzed by liquid-scintillation counting. For every mutant examined, 68−89% of the loaded counts eluted in fractions that correspond to a unique peak of absorbance at 210 nm (A_{210}) (Figure 6A). Differences in mobility for each mutant were consistent with the changes in the hydrophobicity of the substituted residue. Mass spectrometric analysis of the ^{32}P-containing peak from wild-type Sst2 revealed a peptide of the molecular weight predicted for a singly phosphorylated tryptic fragment containing Ser-539 (Figure 6B). The unique A_{210} peak isolated from $Sst2^{H538W}$ exhibited a comigrating peak of tryptophan fluorescence (Figure 6A), consistent with the introduction of a tryptophan residue adjacent to Ser-539. Mass spectrometric analysis of this peak revealed a peptide of the molecular weight predicted for a singly phosphorylated, tryptophan-substituted, tryptic

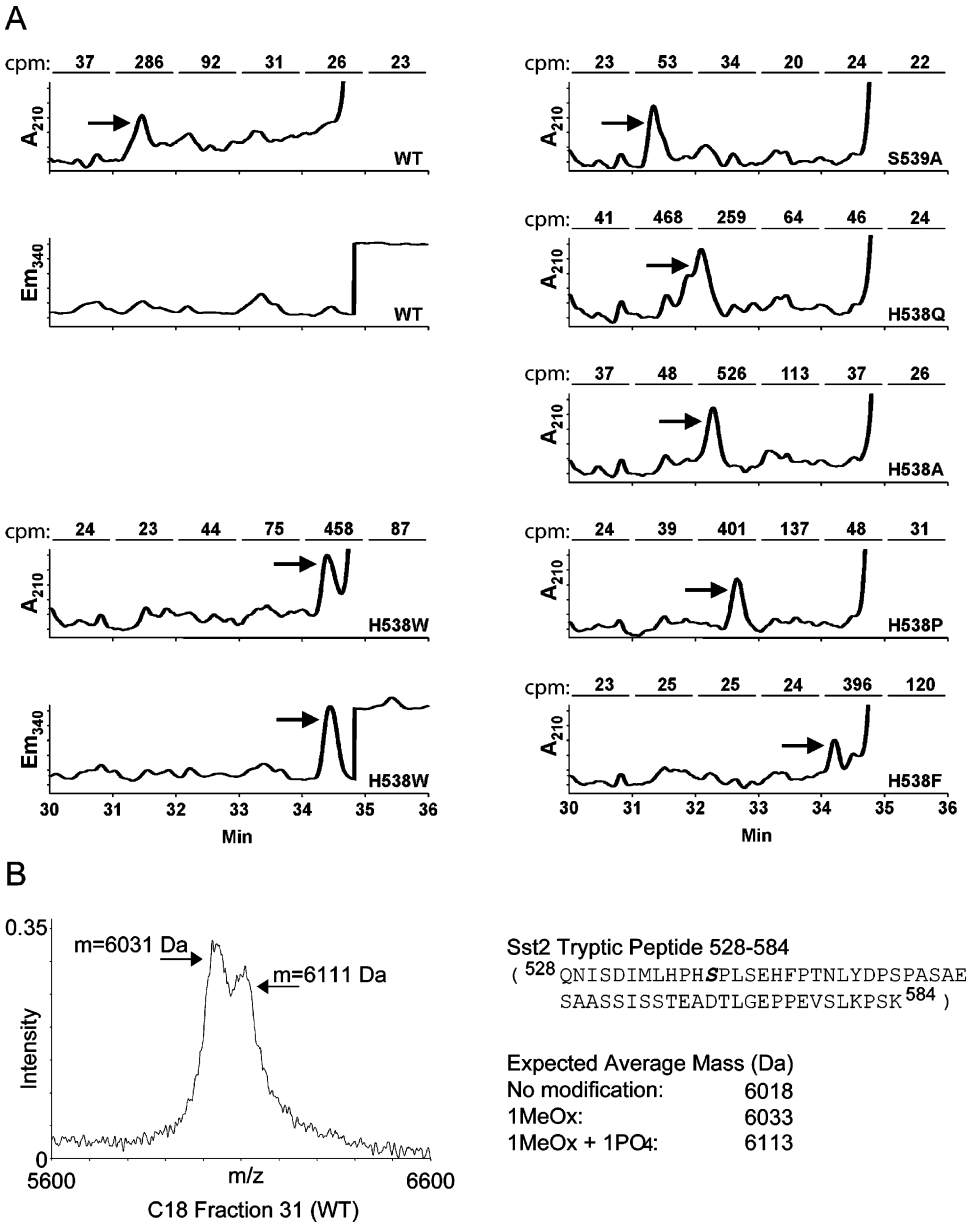

FIGURE 6: His-538 substitutions preserve phosphorylation of Sst2 at Ser-539. (A) To determine if substitutions at His-538 alter the *site* of Sst2 phosphorylation in vitro, ^{32}P-labeled Sst2 fusion proteins were resolved by SDS−PAGE, excised, and trypsinized, and the resulting peptides were fractionated by reverse-phase HPLC. Eluting peptides were monitored by absorbance at 210 nm and by fluorescence spectroscopy (278 nm excitation, 340 nm emission) using an in-line spectrophotometer and fluorometer, respectively. Liquid-scintillation counts (cpm) from each fraction are displayed above the corresponding HPLC chromatogram to demonstrate the coelution of the radioactive peak with the Ser-539-containing tryptic peptide. (B) The identities of the peak fractions containing the Ser-539 tryptic peptide from wild-type (fraction 31) and Sst2^{H538W} (fraction 34, data not shown) were confirmed using linear-mode MALDI-TOF mass spectrometry. The mass measurement from both samples contained a peptide of the predicted average mass of a singly phosphorylated tryptic fragment containing Ser-539.

fragment containing Ser-539 (data not shown). From these results, we conclude that His-538 substitution mutants are phosphorylated at Ser-539. In addition, we conclude that substitution of the −1 residue in the MAP kinase consensus sequence does not affect the ability of Fus3 to phosphorylate Sst2. Rather, changes in the phosphorylation state of Sst2^{H538X} mutants observed in vivo are likely due to other factors such as their relative ability to be dephosphorylated.

DISCUSSION

Protein kinases are generally classified according to their substrate sequence specificity. Among the Ser/Thr kinases, there are at least four distinct functional groups. The largest is the "Arg/Lys-directed" kinases, which strongly prefer a basic amino acid at the −3 position. Members of this group include the calcium/calmodulin dependent kinases, protein kinase C, phosphorylase kinase γ, and the cAMP-dependent protein kinase. A second group prefers acidic or phosphorylated amino acids at the −3 position and is typified by casein kinase I and casein kinase II. A third group prefers hydrophobic residues at the −3 position. Finally, there is a substantial number of "Proline-directed" protein kinases, which prefer substrates with a Pro immediately C-terminal to the target Ser or Thr. This group includes the cyclin-dependent protein kinases as well as the MAP kinases considered here.

The classification of protein kinases based on substrate sequence specificity was established using two broad strate-

gies. One strategy has been to map sites of phosphorylation directly by Edman degradation sequencing and, more currently, by mass spectrometry, and then deduce common sequence elements for that particular kinase. This approach requires knowledge of the kinase responsible for a given phosphorylation event and the ability to purify sufficient quantities of the substrate needed to map the site of modification. Not surprisingly, this has been accomplished in only a handful of cases.

A more common method to determine substrate specificity is to assay phosphorylation of short synthetic peptides, which are usually derived from known protein substrates. This approach allows detailed and quantitative analysis of kinase activity in vitro. However, the phosphorylation of peptides cannot be tested easily in cells. Moreover, peptides are generally very poor substrates. For instance, one of the most commonly used peptide substrates for MAP kinase assays ("ERKtide") displays a 600-fold lower catalytic efficiency (K_{cat}/K_m) than the widely used protein substrate myelin basic protein (*32*). One reason for such discrepancies is that catalytic efficiency depends greatly on the local environment of phospho-acceptor sites. Moreover, peptides are generally more flexible than proteins and may exist only transiently in a conformation suitable for phosphorylation. Another difference is that some kinases require separate docking sites that direct the catalytic site to certain Ser/Thr residues, while others are excluded. Finally, some kinases undergo stimulus-dependent translocation to their site of action, so their activity can depend substantially on proper subcellular localization. Clearly, there are mechanisms that dictate substrate specificity that we do not fully understand and that are not fully conveyed using synthetic peptides.

Both of the strategies described above have been applied in the characterization of MAP kinase substrate specificity. One early study used synthetic peptides derived from myelin basic protein to show that basic (Arg), acidic (Glu), polar (Gln), and nonpolar (Ala, Leu, and Phe) residues are equally tolerated at the −1 position. A second study examined ERK1 and ERK2 phosphorylation of synthetic peptides derived from the EGF receptor, and in this instance, very small differences in the rate of phosphorylation were observed when Leu at −1 was replaced with Lys, Arg, or Glu (*22*). These studies also tested peptide substrates lacking the −1 residue and found them to be poor substrates, suggesting that Pro is disfavored at that position. However, these mutant peptides were also shorter by one residue than the wild-type comparison and, in no case, was a peptide with Pro at both the −1 and −2 positions tested. A third study using random peptide library screening did not uncover any strong preferences by ERK1 for residues at the −5, −4, −3, −1, +2, +3, or +4 positions (*33*, *34*).

While most information is available from analysis of synthetic peptides, MAP kinase phosphorylation sites have been mapped for some proteins. Examination of primary sequences surrounding the phosphorylation sites in known MAP kinase substrates reveals no conservation of residues outside the Pro-X-Ser/Thr-Pro motif (*35*, *36*). At the −1 position, Leu is most frequently present; examples include the very first MAP kinase substrates identified, the epidermal growth factor receptor (*35*), and the proto-oncogenes c-*myc* and c-*jun* (*36*). Other well-characterized substrates contain Arg (myelin basic protein), Thr (tyrosine hydroxylase), or Lys (caldesmon). *Previously there has been no comprehensive analysis of MAP kinase sequence specificity using a native protein substrate*, a situation that prompted us to conduct this analysis.

Here, we have shown that Sst2 is phosphorylated by the MAP kinase Fus3 (Figures 1, 4, and 5). We have also shown that deletion or substitution of the −1 residue fails to diminish Sst2 activity (Figure 2, Table 1) or MAP kinase phosphorylation after pheromone stimulation (Figure 3). We did observe changes in the basal phosphorylation state of some $Sst2^{H538X}$ mutants; however, these differences are not due to changes in their intrinsic ability to serve as Fus3 substrates (Figure 4). More likely, changes in the phosphorylation state of these mutants in vivo is due to other factors, such as their ability to be dephosphorylated. The apparent loss of phosphorylation observed for three mutants, in which His was replaced with Phe, Pro, or Trp, resulted from a loss of the phosphorylation-dependent mobility shift, since all three mutants purified from bacteria were fully active as substrates for Fus3 (Figure 5). These results provide further evidence that perturbation of the −1 position does not affect substrate−kinase interaction.

The approach used here overcomes many of the shortcomings of the two methods outlined above. By selecting a known substrate and systematically replacing a portion of the consensus recognition sequence, we could discern whether a given residue is preferred at a given site. This approach could also be used to determine whether a native sequence confers *optimal* substrate activity for a given kinase. This is important since not all consensus sites within a protein are phosphorylated and not all sites of phosphorylation adhere to the consensus sequence. Even if a residue is commonly found at a particular site, this does not necessarily mean that it confers the best activity. Indeed, there may be situations where a less-than-optimal sequence is most suitable.

It is possible that mutations that alter kinase−substrate recognition may have consequences in vivo that would not be evident in vitro. Ideally, we might address this possibility by metabolic ^{32}P-labeling of the different His-538 mutants. However, there are additional sites of Sst2 phosphorylation (*37*) requiring unknown kinases besides Fus3 (see Figures 5 and 6). Moreover, many of the His-538 mutants exhibit differences in basal phosphorylation (Figure 3). These factors would confound interpretation of ^{32}P incorporation experiments, since total labeling would not accurately reflect previously phosphorylated protein or even Fus3-dependent phosphorylation. It is for these reasons that the mobility shift assay remains the most reliable method to track Ser-539 phosphorylation in vivo, although this analysis is best done in conjunction with in vitro studies using purified kinase and substrate where most external effects can be eliminated.

In summary, we have shown that Fus3 phosphorylates Sst2. In addition, we analyzed the substrate sequence requirements for Fus3 phosphorylation of Sst2. Our data reveal that MAP kinase activity is not constrained by the residue preceding the phospho-acceptor site, in agreement with earlier studies with artificial peptide substrates. Our conclusions are based on a comprehensive and systematic analysis of an established phosphorylation site in Sst2. Presently, we are expanding this analysis to identify other recognition sequences throughout the native protein and in other Fus3 substrates within the pathway. When combined

with studies of protein binding and phosphorylation, a more detailed understanding of substrate specificity should emerge.

ACKNOWLEDGMENT

We thank Beverly Errede, Rick Fishel, Lorena Kallal, and Jason Snyder for providing reagents, as well as Tiffany Runyan Garrison and Lee Graves for providing comments and encouragement.

REFERENCES

1. Dohlman, H. G. (2002) G proteins and pheromone signaling, *Annu. Rev. Physiol. 64*, 129−152.
2. Apanovitch, D. M., Slep, K. C., Sigler, P. B., and Dohlman, H. G. (1998) Sst2 is a GTPase-activating protein for Gpa1: purification and characterization of a cognate RGS-Gα protein pair in yeast, *Biochemistry 37*, 4815−4822.
3. Yi, T. M., Kitano, H., and Simon, M. I. (2003) A quantitative characterization of the yeast heterotrimeric G protein cycle, *Proc. Natl. Acad. Sci. U.S.A. 100*, 10764−10769.
4. Dohlman, H. G., and Thorner, J. W. (2001) Regulation of G protein-initiated signal transduction in yeast: paradigms and principles, *Annu. Rev. Biochem. 70*, 703−754.
5. Elion, E. A., Satterberg, B., and Kranz, J. E. (1993) FUS3 phosphorylates multiple components of the mating signal transduction cascade: evidence for STE12 and FAR1, *Mol. Biol. Cell 4*, 495−510.
6. Breitkreutz, A., Boucher, L., and Tyers, M. (2001) MAPK specificity in the yeast pheromone response independent of transcriptional activation, *Curr. Biol. 11*, 1266−1271.
7. Hung, W., Olson, K. A., Breitkreutz, A., and Sadowski, I. (1997) Characterization of the basal and pheromone-stimulated phosphorylation states of Ste12p, *Eur. J. Biochem. 245*, 241−251.
8. Breitkreutz, A., and Tyers, M. (2002) MAPK signaling specificity: it takes two to tango, *Trends Cell Biol. 12*, 254−257.
9. Cook, J. G., Bardwell, L., Kron, S. J., and Thorner, J. (1996) Two novel targets of the MAP kinase Kss1 are negative regulators of invasive growth in the yeast *Saccharomyces cerevisiae*, *Genes Dev. 10*, 2831−2848.
10. Zhou, Z., Gartner, A., Cade, R., Ammerer, G., and Errede, B. (1993) Pheromone-induced signal transduction in *Saccharomyces cerevisiae* requires the sequential function of three protein kinases, *Mol. Cell. Biol. 13*, 2069−2080.
11. Maleri, S., Ge, Q., Hackett, E. A., Wang, Y., Dohlman, H. G., and Errede, B. (2004) Persistent activation by constitutive Ste7 promotes Kss1-mediated invasive growth but fails to support Fus3-dependent mating in yeast, *Mol. Cell. Biol. 24*, 9221−9238.
12. Bardwell, L., Cook, J. G., Inouye, C. J., and Thorner, J. (1994) Signal propagation and regulation in the mating pheromone response pathway of the yeast *Saccharomyces cerevisiae*, *Dev. Biol. 166*, 363−379.
13. Doi, K., Gartner, A., Ammerer, G., Errede, B., Shinkawa, H., Sugimoto, K., and Matsumoto, K. (1994) MSG5, a novel protein phosphatase promotes adaptation to pheromone response in *S. cerevisiae*, *EMBO J. 13*, 61−70.
14. Tyers, M., and Futcher, B. (1993) Far1 and Fus3 link the mating pheromone signal transduction pathway to three G1-phase Cdc28 kinase complexes, *Mol. Cell. Biol. 13*, 5659−5669.
15. Peter, M., Gartner, A., Horecka, J., Ammerer, G., and Herskowitz, I. (1993) FAR1 links the signal transduction pathway to the cell cycle machinery in yeast, *Cell 73*, 747−760.
16. Cherkasova, V. A., McCully, R., Wang, Y., Hinnebusch, A., and Elion, E. A. (2003) A novel functional link between MAP kinase cascades and the Ras/cAMP pathway that regulates survival, *Curr. Biol. 13*, 1220−1226.
17. Feng, Y., and Davis, N. G. (2000) Feedback phosphorylation of the yeast a-factor receptor requires activation of the downstream signaling pathway from G protein through mitogen-activated protein kinase, *Mol. Cell. Biol. 20*, 563−574.
18. Li, E., Cismowski, M. J., and Stone, D. E. (1998) Phosphorylation of the pheromone-responsive Gbeta protein of *Saccharomyces cerevisiae* does not affect its mating-specific signaling function, *Mol. Gen. Genet. 258*, 608−618.
19. Oehlen, B., and Cross, F. R. (1994) Signal transduction in the budding yeast *Saccharomyces cerevisiae*, *Curr. Opin. Cell Biol. 6*, 836−841.
20. Garrison, T. R., Zhang, Y., Pausch, M., Apanovitch, D., Aebersold, R., and Dohlman, H. G. (1999) Feedback phosphorylation of an RGS protein by MAP kinase in yeast, *J. Biol. Chem. 274*, 36387−36391.
21. Clark-Lewis, I., Sanghera, J. S., and Pelech, S. L. (1991) Definition of a consensus sequence for peptide substrate recognition by p44mpk, the meiosis-activated myelin basic protein kinase, *J. Biol. Chem. 266*, 15180−15184.
22. Gonzalez, F. A., Raden, D. L., and Davis, R. J. (1991) Identification of substrate recognition determinants for human ERK1 and ERK2 protein kinases, *J. Biol. Chem. 266*, 22159−22163.
23. Tesmer, J. J., Berman, D. M., Gilman, A. G., and Sprang, S. R. (1997) Structure of RGS4 bound to AlF4- activated G(iα1): stabilization of the transition state for GTP hydrolysis, *Cell 89*, 251−261.
24. Dohlman, H. G., Song, J., Ma, D., Courchesne, W. E., and Thorner, J. (1996) Sst2, a negative regulator of pheromone signaling in the yeast *Saccharomyces cerevisiae*: expression, localization, and genetic interaction and physical association with Gpa1 (the G-protein α subunit), *Mol. Cell. Biol. 16*, 5194−5209.
25. Gietz, R. D., and Woods, R. A. (2002) Transformation of yeast by the LiAc/ss carrier DNA/PEG method, *Methods Enzymol. 350*, 87−96.
26. Dohlman, H. G., Apaniesk, D., Chen, Y., Song, J., and Nusskern, D. (1995) Inhibition of G-protein signaling by dominant gain-of-function mutations in Sst2p, a pheromone desensitization factor in *Saccharomyces cerevisiae*, *Mol. Cell. Biol. 15*, 3635−3643.
27. Kallal, L., and Fishel, R. (2000) The GTP hydrolysis defect of the *Saccharomyces cerevisiae* mutant G-protein Gpa1(G50V), *Yeast 16*, 387−400.
28. Errede, B., Gartner, A., Zhou, Z., Nasmyth, K., and Ammerer, G. (1993) MAP kinase-related FUS3 from *S. cerevisiae* is activated by STE7 in vitro, *Nature 362*, 261−264.
29. Borchers, C., Peter, J. F., Hall, M. C., Kunkel, T. A., and Tomer, K. B. (2000) Identification of in-gel digested proteins by complementary peptide mass fingerprinting and tandem mass spectrometry data obtained on an electrospray ionization quadrupole time-of-flight mass spectrometer, *Anal. Chem. 72*, 1163−1168.
30. Hoffman, G., Garrison, T. R., and Dohlman, H. G. (2002) Analysis of RGS proteins in *Saccharomyces cerevisiae*, *Methods Enzymol. 344*, 617−631.
31. Hao, N., Yildirim, N., Wang, Y., Elston, T. C., and Dohlman, H. G. (2003) Regulators of G protein signaling and transient activation of signaling: experimental and computational analysis reveals negative and positive feedback controls on G protein activity, *J. Biol. Chem. 278*, 46506−46515.
32. Prowse, C. N., Hagopian, J. C., Cobb, M. H., Ahn, N. G., and Lew, J. (2000) Catalytic reaction pathway for the mitogen-activated protein kinase ERK2, *Biochemistry 39*, 6258−6266.
33. Songyang, Z., Lu, K. P., Kwon, Y. T., Tsai, L. H., Filhol, O., Cochet, C., Brickey, D. A., Soderling, T. R., Bartleson, C., Graves, D. J., DeMaggio, A. J., Hoekstra, M. F., Blenis, J., Hunter, T., and Cantley, L. C. (1996) A structural basis for substrate specificities of protein Ser/Thr kinases: primary sequence preference of casein kinases I and II, NIMA, phosphorylase kinase, calmodulin-dependent kinase II, CDK5, and Erk1, *Mol. Cell. Biol. 16*, 6486−6493.
34. Songyang, Z. (2001) Analysis of protein kinase specificity by peptide libraries and prediction of in vivo substrates, *Methods Enzymol. 332*, 171−183.
35. Northwood, I. C., Gonzalez, F. A., Wartmann, M., Raden, D. L., and Davis, R. J. (1991) Isolation and characterization of two growth factor-stimulated protein kinases that phosphorylate the epidermal growth factor receptor at threonine 669, *J. Biol. Chem. 266*, 15266−15276.
36. Alvarez, E., Northwood, I. C., Gonzalez, F. A., Latour, D. A., Seth, A., Abate, C., Curran, T., and Davis, R. J. (1991) Pro-Leu-Ser/Thr-Pro is a consensus primary sequence for substrate protein phosphorylation. Characterization of the phosphorylation of c-myc and c-jun proteins by an epidermal growth factor receptor threonine 669 protein kinase, *J. Biol. Chem. 266*, 15277−15285.
37. Gruhler, A., Olsen, J. V., Mohammed, S., Mortensen, P., Faergeman, N. J., Mann, M., and Jensen, O. N. (2005) Quantitative phosphoproteomics applied to the yeast pheromone signaling pathway, *Mol. Cell. Proteomics 4*, 310−327.

BI0503091